International Journal of Thermophysics, Vol. 18, No. 2, 1997

Measurements of Thermophysical Properties of Molten Silicon by a High-Temperature Electrostatic Levitator[1]

W. K. Rhim,[2,3] S. K. Chung,[2] A. J. Rulison,[2,4] and R. E. Spjut[5]

Several thermophysical properties of molten silicon measured by the high-temperature electrostatic levitator at JPL are presented. They are density, constant-pressure specific heat capacity, hemispherical total emissivity, and surface tension. Over the temperature range investigated ($1350 < T_m < 1825$ K), the measured liquid density (in $g \cdot cm^{-3}$) can be expressed by a quadratic function, $\rho(T) = \rho_m - 1.69 \times 10^{-4}(T - T_m) - 1.75 \times 10^{-7}(T - T_m)^2$ with T_m and ρ_m being 1687 K and 2.56 $g \cdot cm^{-3}$, respectively. The hemispherical total emissivity of molten silicon at the melting temperature was determined to be 0.18, and the constant-pressure specific heat was evaluated as a function of temperature. The surface tension (in 10^{-3} $N \cdot m^{-1}$) of molten silicon over a similar temperature range can be expressed by $\sigma(T) = 875 - 0.22(T - T_m)$.

KEY WORDS: density; electrostatic levitation; hemispherical total emissivity; molten silicon; specific heat; surface tension.

1. INTRODUCTION

Accurate thermophysical property values of molten silicon are important ingredients in the numerical modeling of crystal growth process. As dimensions of semiconductor devices continue to shrink, needs for high-quality

[1] Invited paper presented at the Fourth Asian Thermophysical Properties Conference, September 5–8, 1995, Tokyo, Japan.

[2] Jet Propulsion Laboratory, California Institute of Technology, 4800 Oak Grove Drive, Pasadena, California 91109, U.S.A.

[3] To whom correspondence should be addressed.

[4] National Research Council Resident Research Associate. Present address: Space Systems/Loral, Palo Alto, California 94303, U.S.A.

[5] Department of Engineering, Harvey Mudd College, Claremont, California 91711, U.S.A.

0195-928X/97/0300-0459$12.50/0

840/18/2-11

crystals are ever increasing, and understanding and controlling the formation kinetics of a variety of crystal defects in a grown crystal are becoming very important.

In this paper, density, specific heat, and surface tension of molten silicon which were measured using the high-temperature electrostatic levitator (HTESL) are presented and discussed. By isolating the sample from container walls, the silicon melt undercooled as much as 300 K. In addition, the hemispherical total emissivity at melting temperature has been evaluated using a known literature value of specific heat capacity at the melting temperature.

The main apparatus used for the present experiments was the HTESL [1] at JPL. The capability of levitating conducting as well as nonconducting materials is unique to this levitator. Since the system operates in a high vacuum, the sample purity is maintained and melts undercools deeply. Some of the characteristics of HTESL which made the present work possible are that (i) it could levitate pure silicon samples, melted them while in levitation, and could reach undercooled states; and (ii) sample heating and levitation do not interfere with each other, so that the sample could be cooled in a purely radiative manner when the heating source was either turned off or blocked. This allowed description of the whole cooling process by a well-defined heat transfer equation. (iii) Levitated drop is quiescent and maintains an axisymmetric shape along a vertical direction. In reality, samples show a slightly prolate spherical shape due to surface charges. Extent of asphericity depends on the apparent surface tension, radius, and mass density of the drop. In the case of a molten silicon 2 mm in diameter, the asphericity was less than 1%.

2. EXPERIMENTAL PROCEDURE

The HTESL levitates a sample 1 to 3 mm in diameter between a pair of parallel-disk electrodes spaced about 10 mm apart. The electrode assembly is housed by a stainless-steel chamber which is typically evacuated to 10^{-8} T before sample heating begins. Samples are heated using a 1-KW xenon arc lamp. Detailed description of the HTESL is given in an earlier publication [1].

Once a levitated sample is molten, the melt shows a very nearly spherical shape due to the action of surface tension. To maintain clean surfaces during processing, it was necessary to begin with pure, clean samples. Silicon samples were prepared from 99.9995% pure stock from Johnson–Matthey. These were then ground roughly into spheres. They were cleaned by immersion in 5% hydrofluoric acid at room temperature for 5 min,

rinsed in distilled water, and finally, rinsed in anhydrous ethanol. The samples weighed approximately 10 mg.

Since the levitation mechanism of HTESL does not affect the sample temperature, a sample that is heated by a radiant heating source will cool purely radiatively when the heating source is blocked; and the ensuing cooling process can be described by the radiative heat transfer equation

$$mc_p \frac{dT}{dt} = -\sigma_{SB}\varepsilon_T A(T^4 - T_E^4) \tag{1}$$

where m is the sample mass, c_p is the constant pressure specific heat capacity, T is the sample temperature, T_E is the environment temperature, σ_{SB} is the Stefan–Boltzmann constant ($5.6705 \times 10^{-8} \mathrm{W \cdot m^{-2} \cdot K^{-4}}$), and ε_T is the hemispherical total emissivity. The fact that accurate measurement of c_p/ε_T is possible from Eq. (1) is one of the most important merits of the HTESL.

Experiments for mass density and specific heat capacity of molten silicon were initiated by blocking the heating source and allowing the silicon melt to cool to undercooled state until the recalescence took place. Upon beam blocking, both temperature measurement by a pyrometer and the image recording by a video system went on simultaneously throughout cooling process. A typical temperature-versus-time profile for a silicon melt obtained during such a cooling process is shown in Fig. 1. The melt started

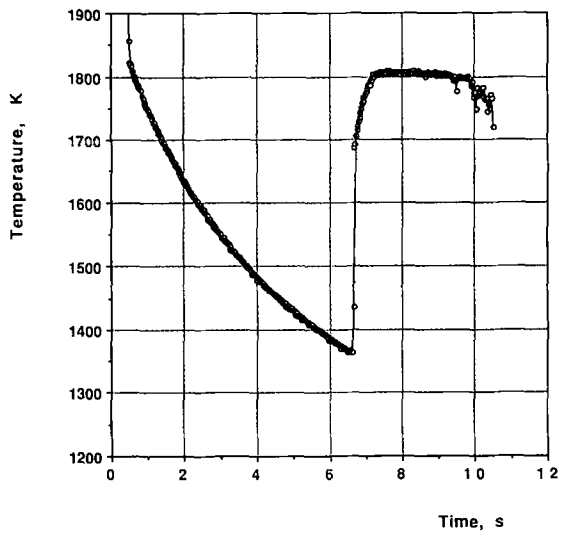

Fig. 1. A typical temperature-versus-time profile for a silicon melt undergoing a purely radiative cooling process.

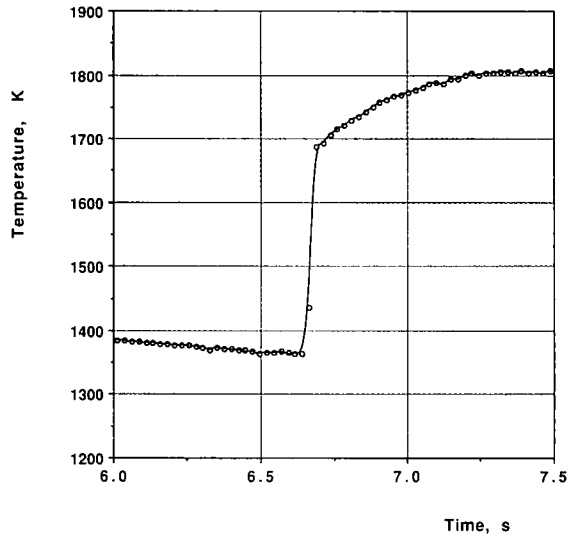

Fig. 2. A magnified view of Fig. 1 around the recaliscence event.

to cool from about 100 K above the melting temperature and undercooled as much as 300 K before recalescence took place. Upon recalescence the sample temperature rose sharply and reached the isotherm state. Unlike many purely metals, Fig. 1 does not show constant radiance over the isotherm region. This is attributed to the changing spectral emissivity in this region. Discontinuities in the temperature gradient due to phase transition is clearly identifiable in the magnified view shown in Fig. 2. Output of the single-color pyrometer operating at 700 nm was calibrated using Planck's spectral distribution of emissive power, taking temperature immediately following the recalescence as its melting temperature ($T_m = 1687$ K). The 700 nm spectral emissivity of the melt over the entire liquid temperature range was assumed to be constant.

Temperature dependence of the sample density was measured by analyzing the video images taken during a cooling process. The sample temperature from the pyrometer was inserted in each video frame so that one can readily make a sample image-vs-sample temperature correlation. The image size was extracted from each video frame using an image analysis method which was recently developed at JPL [2].

For the surface tension measurement, a small sinusoidal electric field was superimposed on the levitation field and the characteristic oscillation was searched by sweeping the frequency. When a resonance is found, the

mode of oscillation was identified and the frequency at the maximum oscillation amplitude was recorded along with the sample temperature.

Surface charge on a levitated drop lowers the actual surface tension, and the drop oscillation frequency should reflect this. If we know the net drop charge and measure the lowest resonant oscillation frequency, one can use the Rayleigh's expression for charged drop oscillation angular frequency ω to extract the true surface tension σ [3],

$$\omega = \left[\frac{8\sigma}{\rho r_0^3} \left(1 - \frac{Q^2}{16\pi r_0^3 \sigma} \right) \right]^{1/2} \tag{2}$$

where ρ is the mass density of the melt, r_0 is the radius of the melt when it is in spherical shape, and Q is the net sample charge. Effects on surface tension due to nonuniform charge distribution and deviation from a perfect spherical shape were corrected using the perturbational analysis of electrostatically levitated drops by Feng and Beard [4].

3. MASS DENSITY MEASUREMENT

The basic approach used for the density measurements consisted of (i) digitization of the recorded video image, (ii) edge detection, (iii) calculation of the area (therefore, the volume of the sample) through linear spherical harmonic fit, and (iv) calibration of data with respect to a reference sphere for absolute values. The density is then obtained using the sample mass which was measured immediately following the experiment. Detailed description of the image analysis method used in this experiment will be published elsewhere [2].

Figure 3 shows the result of our density measurements of molten silicon over a 400 K span. Unlike pure metals, it shows a quadratic nature which can be fit by the following equation:

$$\rho(T) = \rho_m - 1.69 \times 10^{-4}(T - T_m) - 1.75 \times 10^{-7}(T - T_m)^2 \tag{3}$$

where $\rho(T)$ is the density in $g \cdot cm^{-3}$, the melting temperature $T_m = 1687$ K, and the density at the melting temperature $\rho_m = 2.56\ g \cdot cm^{-3}$. The accuracy of our measurement is estimated to be $\sim 0.5\%$. It is interesting to see from Eq. (3) that, while the density at the melting temperature agrees with a reference value of $2.53\ g \cdot cm^{-3}$ [5] within 1.2%, $(\partial\rho/\partial T)_P$ at T_m is $-1.69 \times 10^{-4}\ g \cdot cm^{-3} \cdot K^{-1}$, which is more than two times smaller in magnitude compared to the reference value of $-3.5 \times 10^{-4}\ g \cdot cm^{-3} \cdot K^{-1}$ given in Ref. 6. This reference did not provide the range of variation among various data. Sasaki et al. [7] reported their observation of an abrupt rise

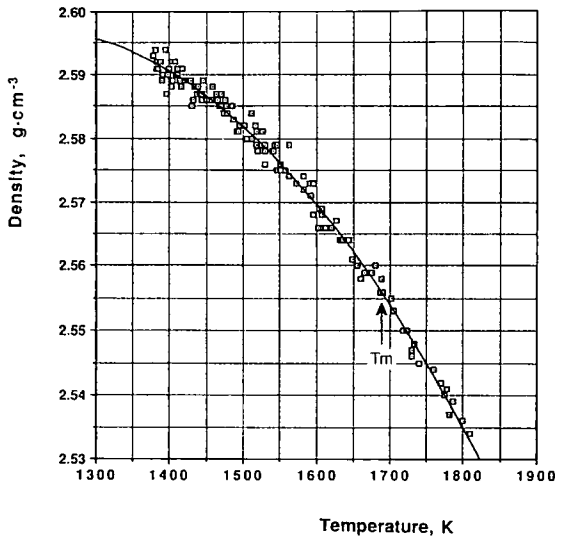

Fig. 3. Density of molten silicon as a function of temperature.

of liquid density in a temperature range below 1700 K with $(\partial\rho/\partial T)_P = -7.6 \times 10^{-4}\ \mathrm{g \cdot cm^{-3} \cdot K^{-1}}$. However, we have not observed such behavior outside the noise level of 0.2%.

One can speculate the meaning of the quadratic behavior of the present density result and relate it to the formation of a short-range order in the undercooked region. In the case of molten pure metals, both density and specific heat tend to show linear behavior. Considering the fact that silicon has a lower density in the solid phase than in liquid, the density of the undercooked liquid will be lowered as a more solid-like tetrahedral order based on double bonds increases. Increasing short-range order is also reflected in the rising specific heat (Fig. 5) with increased undercooling. A fraction of the nonmetallic structure in the undercooked melt may be drawn from such nonlinearity. Detailed analysis related to this topics will be published elsewhere.

4. SPECIFIC HEAT MEASUREMENT

Thermodynamic parameters in the undercooked region carries special implications for the studies of solidification processes and the selection of metastable phases. The constant-pressure specific heat capacity is a very important thermodynamic parameter from which other parameters, such as

the enthalpy, entropy, and Gibbs free energy, can be derived. In spite of their importance, the specific heat capacity and hemispherical total emissivity are known for very few high-temperature liquids. Data are particularly scarce for the undercooked liquids since they immediately solidify when placed in contact with most crucibles. The HTESL allows determination of c_p/ε_T in a simple heat transfer environment while the levitated melt cools to undercooked states. Rearrangement of Eq. (1) gives

$$\frac{c_p}{\varepsilon_T} = -\frac{\sigma_{SB} A (T^4 - T_E^4)}{m(dT/dt)} \tag{4}$$

Using a temperature–time profile obtained experimentally (such as shown in Fig. 1), and evaluating dT/dt from it, c_{pl}/ε_T can be readily obtained as shown in Fig. 4. From this ratio $c_p(T)$ can be determined if $\varepsilon_T(T)$ is known, and conversely, $\varepsilon_T(T)$ can be found if $c_p(T)$ is known [8].

Frequently, specific heat values are known for many materials at their melting temperature, while the values for hemispherical total emissivity are not. In such cases, $\varepsilon_T(T_m)$ at the melting temperature can be obtained. The literature value of the constant-pressure specific heat capacity of molten silicon at the melting temperature is 25.61 $J \cdot mol^{-1} \cdot K^{-1}$. With this value together with the c_{pl}/ε_T obtained from Fig. 4, the hemispherical total emissivity at the melting temperature $\varepsilon_T(T_m)$ becomes 0.18. There are very few published data to which the present value can be compared. However,

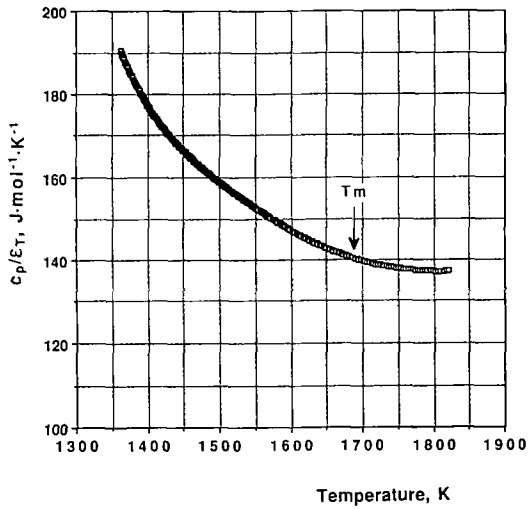

Fig. 4. c_{pl}/ε_T vs temperature of molten silicon as calculated from data shown in Fig. 1.

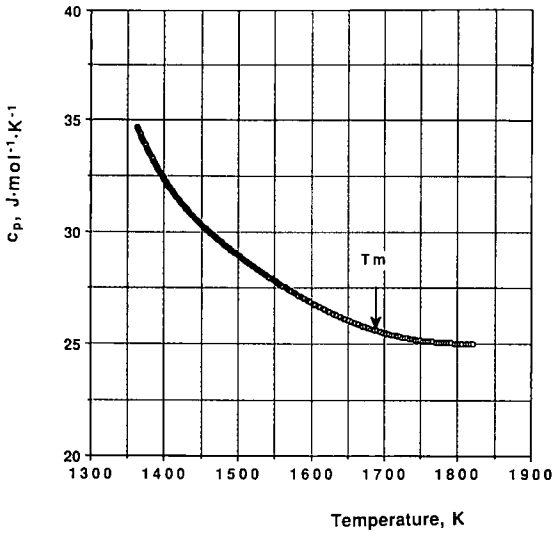

Fig. 5. $c_p(T)$ vs temperature calculated from the result shown in Fig. 4 assuming that $\varepsilon_T(T) = \varepsilon_T(T_m) = 0.18$.

our earlier result [8] showed $\varepsilon_T(T_m) = 0.17 \pm 0.01$ which is in good agreement with the present result.

Strictly speaking, $\varepsilon_T(T)$ has to be independently measured as a function of temperature to evaluate $c_p(T)$. Since $\varepsilon_T(T)$ is not available at the present time, let us assume that it remains constant at $\varepsilon_T(T_m) = 0.18$ throughout the liquid region and extract $c_p(T)$ from Fig. 4 over the same temperature region. There is no basis of such an assumption except that the spectral emissivities of molten silicon measured by Khrisnan et al. [9] at a 640-nm wavelength showed no temperature dependency. Figure 5 shows $c_p(T)$ as a function of temperature so obtained. A nonlinearly decreasing trend of $c_p(T)$ with rising temperature seems to be a characteristic of molten silicon, which contrasts with the rather linear behavior shown by many pure metals [8, 10].

5. SURFACE TENSION

The spherical shape of the melt levitated by the HTESL greatly simplifies the surface tension measurements. In view of the fact that surface tension is particularly sensitive to even minute surface contamination, the HTESL operating in a high-vacuum environment would be ideal for measuring surface tension, particularly of chemically reactive materials.

Unlike experiments described earlier, for the surface tension experiments we had to fix the sample temperature at a predetermined value until the surface tension data at that temperature was obtained. The pyrometer used for this experiment operated at a 4-μm wavelength to avoid interference from the xenon arc-lamp radiation.

Figure 6 shows our surface tension result on molten silicon as a function of temperature. The data could be fit by

$$\sigma(T) = 875 - 0.22(T - T_m) \tag{5}$$

where $\sigma(T)$ is the surface tension in 10^{-3} N $\cdot$ m^{-1}. This result shows the surface tension at the melting temperature to be 875×10^{-3} N $\cdot$ m^{-1}, which is comparable to the 885×10^{-3} N $\cdot$ m^{-1} obtained by Hardy [11] using the sessile drop method. However, it is much greater than the 783.5×10^{-3} N $\cdot$ m^{-1} obtained by Pryzborowski et al. [12] using the electromagnetic levitation method. As for $d\sigma(T)/dT$, the present result shows 0.22×10^{-3} N $\cdot$ m^{-1} $\cdot$ K^{-1}, while Refs. 11 and 12 showed 0.28×10^{-3} and 0.65×10^{-3} N $\cdot$ m^{-1} $\cdot$ K^{-1}, respectively. At the present time, it is premature to prefer a particular result over others. Only more comprehensive experimental conditions in each of various experimental approaches would be able to reveal causes of such different results.

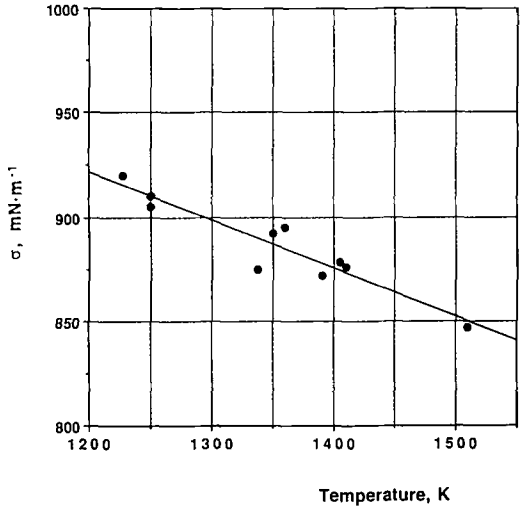

Fig. 6. Surface tension $\sigma(T)$ of molten silicon as a function of temperature.

6. DISCUSSION

We have presented data on the density, hemispherical total emissivity, constant-pressure heat capacity, and surface tension of molten silicon over a 400 K temperature range around the melting point. These measurements were performed for the first time using the HTESL which was recently developed at JPL. Levitated molten silicon sample was stable in its position as well as in its shape, and the sample shape was a prolate spheroid with its symmetry axis along the gravity axis. (The vertical axis was approximately 1% longer than the horizontal axis.) Such a simple sample shape greatly simplified the density measurement process since it required analysis of only one side-view image to find the density at a given temperature. Furthermore, the spherical sample shape also simplified the surface tension measurement through detection of the only fundamental resonance frequency at a given temperature since all five possible modes ($m = 0, \pm 1, \pm 2$) are degenerate when the shape is spherical. We have also shown that the use of purely radiative cooling process increased the accuracy of c_{pl}/ε_T as a function of temperature.

There are areas which need to be improved. For instance, the oscillating electric field which induced the resonance frequency could have been abruptly removed and observed the ensuing decay signal. Clearly, such a signal can be considered as a free-decay signal, and the frequency can be related to the surface tension, and the decay constant can be related to the viscosity.

As a final note, we would like to mention that the present capability of the HTESL can be extended further with additional capabilities of measuring spectral as well as hemispherical total emissivities, thermal conductivity, and electrical conductivity. Development of such capabilities is under way.

ACKNOWLEDGMENTS

The authors would like to thank Mr. Daniel Barber for various technical assistance throughout the work, Dr. E. Trinh for bringing J. Feng's work to their attention, and Dr. D. Witter at Texas Intruments Inc. for bringing the paper by Pryzborowski et al. to their attention. This work was carried out at the Jet Propulsion Laboratory, California Institute of Technology, under contract with the National Aeronautical and Space Administration.

REFERENCES

1. W. K. Rhim, S. K. Chung, D. Barber, K. F. Man, G. Gutt, A. Rulison, and R. E. Spjut, *Rev. Sci. Instrum.* **64**:2961 (1993).
2. S. K. Chung, D. Thiessen, Y. J. Kim, and W. K. Rhim, *Rev. Sci Instrum.* **67**:3175 (1996).

3. J. W. S. Rayleigh, *Phil. Mag.* **14**:184, (1882).
4. J. Q. Feng and K. V. Beard, *Proc. R. Soc. Lond. A* **430**:133, (1990).
5. V. M. Glazov, S. N. Chizhevskaya, and N. N. Glagoleva, *Liquid Semiconductors* (Plenum Press, New York, 1969), p. 61.
6. T. Iida and R. I. L. Guthrie, *The Physical Properties of Liquid Metals* (Clarendon Press, Oxford, 1988), p. 71.
7. H. Sasaki, E. Tokizaki, K. Terashima, and S. Kimura, *Jpn. J. Appl. Phys.* **33**:3803 (1994).
8. A. J. Rulison and W. K. Rhim, *Metallurg. Mater. Trans. B* **26B**:503 (1995).
9. S. Krishnan, J. K. R. Weber, P. C. Nordine, R. A. Schiffman, R. H. Hauge, and J. L. Margrave, *High Temp. Sci.* **30**:137 (1991).
10. A. J. Rulison and W. K. Rhim, *Phys. Chem. Liquids* **30**:169 (1995).
11. S. C. Hardy, *J. Crystal Growth* **69**:456 (1984).
12. M. Pryzborowski, T. Hibiya, M. Eguchi, and I. Egry, *J. Jpan. Assoc. Crystal Growth* **21**(3):224 (1994).